2015

Infection and Dissemination of TaV-GFP Tagged Sindbis in Aedine Mosquitoes and Cell Lines

Jason J. Saredy

Infection and Dissemination of TaV-GFP Tagged Sindbis

in Aedine Mosquitoes and Cell Lines

By

Jason Jonathan Saredy

A thesis submitted to the Department of Biology

in partial fulfillment of the requirements for the degree of

Master of Science in Biology

UNIVERSITY OF NORTH FLORIDA

COLLEGE OF ARTS AND SCIENCES

April, 2015

The thesis of Jason Jonathan Saredy is approved: Date

_____   _____

Dr. Doria F. Bowers

_____   _____

Dr. Gregory Ahearn

_____   _____

Dr. Paul Linser

Accepted for the Biology Department:

_____   _____

Dr. Daniel Moon
Chair

Accepted for the College of Arts and Sciences:

_____   _____

Dr. Barbara Hetrick
Dean

Accepted for the University:

_____   _____

Dr. John Kantner
Dean of the Graduate School

Acknowledgements

I would like to thank my mentor Dr. Bowers for putting up with all the antics that accompany accepting a physicist into a biology lab over the past several years. Her support of my interests started during my undergraduate and continued through my masters, always keeping me striving while at times having to smack me back on track. My committee members Dr. Ahearn and Dr. Linser for their guidance through the process and willingness to bring me into their labs to help put out various fires.

I would like to also thank the various lab mates: Kristen Ciano and Erica Kelly for providing a role model of researchers, Zoe Lyski for providing a constant source of frustration and pushing me to actually do work that applies to my thesis instead of just playing with new ideas in the lab, Florence Chim for providing someone to throw ideas off of and an extra hand.

My parents for driving me to look for higher education and keeping me on track, no matter how much of a pain I was I knew I always had a safe haven to go home and unwind.

Special thanks to my wife. She has stood by my side since the first moment I got the itch to jump fields into biology. She put up with the many long nights, barely being home between working full-time, the lab, and the Army. She never feared when the stack of papers on my desk started to stack up, the random paper being thrown across the apartment and angry remarks about a particularly bad student, and occasional binge drinking after a long day of dissections.

Table of Contents

List of Figures and Tables

Figure 1. (A) The unmodified parental SINV and (B) modification by insertion of expression protein and TaV 2A-like protease. (C) Genomic structure around the insertion site showing the capsid autoprotease and TaV 2A-like protease sequence. (Sun et al., 2014)

Figure 2. Fluorescent confocal images of C7-10 cells (Column I) and C6/36 cells (Column III) infected with SINVTaV-GFP at 0 hr, 6 hr, 12, and 48 hr p.i. Column II and Column IV bright field overlay, respectively. 100µm scale bar.

Table 1. Percentage of infected cells versus total number of cells in C7-10 and C6/36 cells with both stock TR339 TaV-GFP and passaged TR339 TaV-GFP. Measurements were taken at a random selection of 10 100x100µm regions for each treatment.

Table 2. Titration of virus replication and expression of GFP for eGFP-TR339-TaV over 5 passages in BHK-21 cells. (+) indicates presence of GFP in infected cells.

Figure 3. Fluorescent confocal image (A) and bright field overlay (B) of a virus plaque in BHK-21 cells at 18 hours p.i. Plaque is visualized by expression of GFP in infected cells surrounded by clear uninfected cells. 100µm scale bar.

Figure 4. Fluorescent confocal image with LSM overlay of infected C7-10 cells pre (A) and post (B) fixation in 4% paraformaldehyde. 100µm scale bar.

Figure 5. Fluorescent confocal images of paraformaldehyde fixed infected C7-10 cells before (A) and after (B) treatment of 30 minute continuous scanning with 488nm Argon laser. 100µm scale bar.

Figure 6. Fluorescent confocal image of paraformaldehyde fixed infected C7-10 cells before (A) and after (B) treatment of 20 hour scanning with 488nm Argon laser every 30 minutes. 100µm scale bar.

Figure 7. Fluorescent confocal image (A) and bright field overlay (B) of paraformaldehyde fixed infected C7-10 cells after 72 hours of access to direct sunlight. 100µm scale bar.

Figure 8. Semithin cross-section of AMG for nonblooded (A), bloodfed (B), and viremic bloodfed (C). Basal surface of the AMG is covered with longitudinal muscle segments. Differential staining of cells can be seen in the nonblooded and bloodfed segments. Bloodfed AMG is significantly distended when compared to nonblooded AMG. There is an increased disorganization in microvilli caused by this distention. Microvillar height is also noted to be longer than the classic brush border found in other digestive epithelial tissue.

Figure 9. Semithin cross-section of PMG for nonbloodfed (A), bloodfed (B), and viremic bloodfed (C). Basal surface of the PMG is covered with longitudinal and circular muscle segements. There is a noticeable distention of the PMG in response to a bloodmeal.

Additionally there is appears to be a lack in relaxation of muscle segments in response to the viremic bloodmeal. Microvillar height is noted to be longer than the classic brush border. The microvilli also show disorganization in bloodfed PMG when compared to nonbloodfed PMG.

Figure 10. Semithin cross-section of hindgut (HG) for nonbloodfed (A), bloodfed (B), and viremic bloodfed (C). A classic brush border appearance of microvilli is visible which supports the function of the hindgut as mainly expulsion instead of digestion. Circular and longitudinal muscle bands are visible as well has some tracheoles. Malpighian tubule cross-sections and ovaries are visible along the edges of the images. There is little visible difference between nonbloodfed and bloodfed HG.

Figure 11. STEM cross-section of *Ae. aegypti* midgut. (A) Low magnification image showing cross section from lumen (L) to the basement membrane (MB) with several longitudinal muscle bundles (M) and trachea (T). (B) Heavy distribution of microvilli line the lumen of midgut epithelial cells. (C) Basal lateral aspect showing basal infoldings deep into the cells and thick electron-dense BM.

Table 3. Average length of microvilli and inner circumferential length in PMG across nonbloodfed, bloodfed, and viremic bloodfed treatments. Inner circumferential length measured according to interface between microvilli and luminal membrane.

Figure 12. Electronmicrograph of the basal lamina surface (hemolymph) of *Ae. albopictus* midgut. Prominent tracheoles, as well as circular and longitudinal muscle bands are visible. Whole-mount fresh tissue without chemical fixation was observed. Images were taken at 10kV using a large field detector (LFD) at a chamber pressure of 0.974 torr and room temperature. Insert is a higher resolution image demonstrating the branching of the tracheoles into small diameter tracheoles and circular muscle fiber.

Figure 13. Semithin cross-section of *Ae. aegypti* PMG for nonblooded (A-C), bloodfed (D-F), and viremic bloodfed (G-I). Stained with methylene blue and imaged with LSM. Differentially stained cells are noted more in the nonblooded guts while the blooded guts appear more distended. Viremic bloodfed guts are more heavily infolded and lumen collapsed compared with mock bloodfed. Scalebar is 100µm.

Figure 14. Semithin cross-section of *Ae. albopictus* PMG from nonblooded (A-C), bloodfed (D-F), and viremic bloodfed (G-I) adult female mosquitoes. Stained with methylene blue and imaged with LSM. Scalebar is 100µm.

Table 4. Dissemination based on leg assay from TR339 stock infected *Ae. aegypti* and *Ae. albopictus*. No data for days 9 and 12 with *Ae. albopictus*.

Figure 15. Fluorescent confocal image of *Ae. aegypti* midgut infected with SINVTaV-GFP at day 3 p.i. Localized foci of infection is observed in MG epithelial cells. 100µm scale bar.

Abstract

Arthropod-borne-viruses (arboviruses) pose a global threat due to their ability to be
transmitted by hematophagous insects to vertebrate hosts resulting in a range of serious
infectious diseases. Sindbis virus (SINV) is the prototype arbovirus of the genus
Alphavirus in the family Togaviridae. The purpose of this study was to investigate the
use of a fluorescent tagged reporter virus in both *in vitro* and *in vivo* environments. The
fluorescent protein GFP was inserted between the Capsid and PE2 in the genome of
TR339; SINV TaV-GFP (Wm. Klimstra Lab). This virus construct should have the same
infectivity and virulence as wild type TR339, leaving a fluorescent 'path' in infected cells
that may reveal virus transit. Virus stocks were grown in BHK-21 vertebrate cells and
C7-10 mosquito cells. Two *Aedes albopictus* mosquito cell lines, C7-10 and C6/36, were
then challenged with vertebrate and mosquito grown reporter virus. Evidence of GFP
were seen as early as 6 hours post infection (p.i.) in all samples. Infected C7-10 cells with
the vertebrate grown reporter virus were fixed for 1 hour in chilled 4% buffered
paraformaldehyde; GFP was shown to be resilient to both fixation and light quenching.
Ultimately, *Ae. aegypti* mosquitoes were challenged with a viremic bloodmeal at a titer of
10^7 PFU/ml and midguts were dissected over several days. The presence of GFP was
observed in midgut columnar epithelial cells as early as day 3 p.i. and remained localized
even at day 30 p.i. This is in agreement with published work on the interaction of TR339
in *Ae. aegypti* gut, signaling this viral construct as a means to visualize wild-type
infection.

Chapter 1: Introduction

Arthropod-borne viruses (arboviruses) pose a global threat due to their ability to be transmitted by mosquitoes and ticks to vertebrate hosts resulting in a range of serious human and animal diseases (Strauss and Strauss, 1994). Sindbis virus (SINV) is an arbovirus of the genus Alphavirus in the family *Togaviridae*. SINV is a positive sense single, stranded RNA virus that was isolated from *Culex* species mosquitoes collected in a CO_2 trap in Sindbis, Egypt in 1952 (Taylor et al., 1955). Female mosquitoes are the primary biological vectors of the virus. The virus is imbibed during a bloodmeal, which is required by female mosquitoes in order to enrich their eggs with protein and cholesterol for egg maturation (Clements, 1996).

The SINV genome is ~11.7kb and codes for 4 nonstructural proteins (NSP1-4) and 3 structural proteins; capsid (C), and the envelope proteins E1 and E2 (McKnight et al., 1996). Genes for these structural proteins are located in an open reading frame and following translation, are proteolytically cleaved to form C, PE2, 6K, and E1. The C-protein is cleaved via an autoprotease and then PE2 and E1 are co-translationally inserted into the membrane of the endoplasmic reticulum where they are separated. The precursor protein, PE2 is then cleaved into matured E2 and E3, the latter is discarded. C-protein and +RNA progeny genome are then assembled into an icosahedral capsid, surrounded by E1 and E2, and enclosed into a host-derived membrane bilayer (Watson et al., 1991). The variant of SINV used in this investigation is the strain TR339. This strain is generated by the transfection of the ancestral strain AR339 into BHK cells (McKnight et al., 1996). This consensus sequence TR339 eliminates cell culture-adapted mutations that are present in laboratory strains of AR339 (Klimstra et al., 1998).

Arbovirus transmission can occur either horizontally or vertically. In both cases, the mosquito will take in a viremic bloodmeal from an infected vertebrate. For a vertical transmission, the virus crosses from the gut into the ovaries, leading to infected male and female progeny mosquitoes. In a horizontal transmission, the virus must make it from the gut to the salivary glands. This allows the virus escape in the mosquito spit, thereby infected the next vertebrate the permissive mosquito bites. Horizontal transmission is the main route of transmission for SINV. Additionally, humans are a dead end host for SINV as the viremia is too low a titer to cause an infection for subsequent mosquitoes that feed on an infected human.

For SINV transmission, virions imbibed during the blood feeding must first cross the midgut via infection and/or paracellular transport, the gut-infection barrier, and next cross the gut-escape barrier to enter the hemolymph (Chamberlain and Sudia, 1961, Hardy et al., 1976). The mosquito midgut is a simple columnar epithelium surrounded by a basement membrane, muscle bundles (Bowers et al., 1995), nerve fibers (Brown et al., 1985), and tracheoles (Romoser et al., 2004). Paracellular transport could occur from the structural changes the gut undergoes during engorgement on a bloodmeal creating gaps that may act as a by-pass mechanism, a 'leaky gut' (Houk, 1977). Following infection with SINV via an intrathoracic route, virus was identified in midgut associated muscles, but not in the muscles surrounding the ovaries. Ultrastructural difference in cell-to-cell junctions and basal lamina, were identified between the midgut and ovaries (Vo et al., 2010). Evidence of paracellular route was not supported.

In order for a disseminated infection to occur, the virus must penetrate the luminal interface between the bloodmeal and the midgut cells. The bloodmeal typically has three

barriers to reach the apical cell surface composing the gut-infection barrier. First is a peritrophic matrix (PM) that prevents direct contact of the viremic bloodmeal with the epithelial layer (Okuda et al., 2007). Secondly the columnar cells that make up the midgut are covered with microvilli including a complex microvilli-associated network (MN) further separating virions in the infectious bloodmeal from direct contact with the apical aspect of the epithelial layer (Zieler et al., 2000). Third is the epithelial cell entry and amplification (Abell and Brown, 1993).

It has been noted that there are a variety of luminal surface characteristics in midgut cells. While the majority (99-99.9%) of midgut cells are heavily microvilliated, there are cells that are relatively bare of microvilli. The spatial frequencies of these cells are uniform throughout the midgut except for a complete absence in the extreme posterior end (Zieler et al., 2000). Work with malaria shows that these cells appear to be similar to those shown susceptible to being invaded by the parasite (Shahabuddin and Pimenta, 1998, Zieler et al., 1998). It may be possible that the absence of the microvilli, and thus the MN, allows direct contact between the virions in the bloodmeal and the luminal surface of the midgut cells.

These dissemination pathways were attempted to be visualized directly in this study. One difficulty in visualizing the spread of an arbovirus infection is in locating the virus itself. Typically this is accomplished via immunochemistry where an antibody to the virus is used in conjunction with a secondary antibody labeled with a fluorochrome such as Fluorescein isothiocyanate (FITC) or directly visualized with transmission electron microscopy. Utilizing immunochemistry in a living host can be difficult. Several variations of an expression virus have been developed in order to ease this process. Initial

3

work for this study displayed some promise looking directly at the morphology of the gut but was moved towards testing of these expression viruses.

One method is inserting the fluorescent gene with a double promotor in a non-coding region of the genome. An example of a double promoter tag was done with SVHR, a heat resistant variant of AR339, with a green fluorescent protein (GPF) downstream of E1 from the Brown lab at North Carolina State University (Wang, 2008). Since SINV is a single stranded RNA virus, it is prone to high mutation rates making the large complex required for a double promoter tag to lose the expression tag within the first few infection cycles. Tagging upstream of the authentic subgenomic promoter in Venezuelan equine encephalitis virus has been done with some success as well (Caley et al., 1999) but still has the same retention problem. By tagging upstream allows for the expression of the fluorescent tag prior to the translation of structural proteins.

Smaller additions directly to a structural can be made such as fusion of mApple and Venus fluorescent proteins to E2 while retaining the functional structure of E2 (Tsvetkova et al., 2013). This should retain a functionally similar virus that will not as readily lose the fluorescent tag. Tsvetkova and colleagues (2013) found, that while infectivity remained at similar levels to wild type SINV, the two fluorescent-tagged viruses displayed varying cell entry behavior when investigated at the single-particle level.

This study used a different virus construct for monitoring the spatial-temporal characteristics of SINV infection. This expression virus was designed via insertion of a GFP gene between capsid and E2 with the autoprotease on the 3' end of the insert. *Thosea asigna* virus (TaV) 2A-like protease is inserted at the 5' end between the

expression contruct and E2 (Fig 1) (Sun et al., 2014). This setup when used with a small

expression protein (<750 nucleotides) better retains the expression protein. The structural

proteins are unchanged between the expression virus and wild-type TR339. This lead to

the expression of the reporter protein closely mimicking the infection of the unmodified

virus (Sun et al., 2014).

Graphic redacted, paper copy available upon request to home institution.

Figure 1. (A) The unmodified parental SINV and (B) modification by insertion of

expression protein and TaV 2A-like protease. (C) Genomic structure around the insertion

site showing the capsid autoprotease and TaV 2A-like protease sequence. (Sun et al.,

2014)

Mosquito models used were *Aedes aegypti* and *Aedes albopictus*, the Yellow

Fever mosquito and Asian Tiger mosquito, respectively. Both species are endemic to the

United States and coexist in many urban areas of Florida (Alto et al., 2003). The native

species *Ae. aegypi* has been steadily declining as the invasive *Ae. albopictus* continues to encroach into both rural and suburban areas (O'Meara et al., 1995, Alto et al., 2003, Gratz, 2004). Therefore *Ae. albopictus* is speculated to become the principle vector of arboviruses in the world (Moore 1997). Both species are susceptible hosts to SINV and provide a competent lab arbovirus-host system.

Chapter 2: Methods and Materials

Vertebrate cell culture

Cultured BHK-21 cells were grown at 37ºC, 5% CO_2 in enriched minimal essential media (EMEM) supplemented with 10% fetal bovine serum, 5% tryptose phosphate broth, and 20µg/ml Gentamycin. Confluent cell monolayers were lifted with 0.25% Trypsin, passaged and maintained in 25cm^2 flasks until needed.

Invertebrate cell culture

Cultured C7-10 and C6/36 (*Ae. albopictus*) larval cells (Singh, 1967) were grown at 28ºC, 5% CO_2 in EMEM supplemented with 10% fetal bovine serum, 5% tryptose phosphate broth, and 20µg/ml Gentamycin. Cells were split and passaged when confluent monolayers were present and maintained in 25cm^2 flasks until needed.

Expression virus

Expression virus, TR339 TaV-eGFP, was provided by William Klimstra's lab, University of Pittsburg. The reporter protein eGFP gene sequence was inserted as a fusion capsid reporter to wild type SINV strain TR339. The first five amino acids of E3 were inserted in frame to the reporter and the reporter followed by *Thosea asigna* virus (TaV) 2A-like protease. This creates a reporter protein in frame with a leading capsid auto-protease and trailing TaV 2A-like protease which allows the cleavage of the reporter protein in the cytoplasm of the infected cell leaving the constructed progeny virus identical to wild type TR339.

Virus infection of invertebrate cell lines

Cultured C7-10 and C6/36 cells were grown in Nunc® Lab-Tek® 2 chamber slides (http://www.sigmaaldrich.com/catalog/product/sigma/c6682?lang=en&region=US). Daily rocking was required for C7-10 cells to avoid clumping. Pre-confluent cells were challenged with 100µl of 10^7 plaque forming units (PFU)/ml expression virus at a multiplicity of infection (MOI) of 0.1 for 1 hour at room temperature (RT).

Serial virus passage

Cultured BHK-21 cells were grown to pre-confluence in 25cm^2 flasks. A 200µl dilution of expression virus was allowed to be adsorbed for 1 hour at RT and washed in PBS-D to remove inoculum, then replaced with 3ml of cell media, EMEM. Virus was incubated for 24 hours; the media was harvested from the flask, and spun down at 2000 rpm (36 G) for 10 minutes. Passaged virus progeny was collected in the supernatant and titration via plaque assay on BHK-21 cells was performed in parallel of the passage being repeated. For each passage 200µl of undiluted virus medium was utilized to model *in vivo* behavior. This was repeated for a total of 5 passages.

Double overlay plaque assay

Cultured BHK-21 cells were grown to pre-confluence in 25cm^2 flasks. Pre-confluent monolayers were challenged with 200µl of known dilutions of virus. Inoculum was removed and cells covered in a 1:1 mixture of 2X MEM and 2% agarose and incubated for a further 48-60 hours. For expression virus, at 6-12 hr post-infection (p.i.)

flasks were surveyed for GFP as the start of a plaque will be evident as small foci of GFP labeled cells. Once visible plaques are observed a neutral red 1% agarose solution is overlaid as a second layer and further incubated for 12 hours. A plaque is identifiable by a localized clearing or plaque that consists of lysed cells (Hernandez et al., 2005). Plaques were counted and titer calculated via converting number of plaques at known dilution to stock plaque forming units per ml (PFU/ml).

Light-challenge of infected invertebrate cells

TR339 TaV-eGFP infected C7-10 cells in Nunc® Lab-Tek® 2 chamber slides at 72 hr p.i. were fixed in 4% paraformaldehyde in Na cacodylate buffer at 7.4 pH for 30 minutes at RT. Cells were observed immediately following fixation, imaged continuously for 30 minutes, and then imaged every 30 minutes over 24 hours. The culture well plate was then left on a windowsill in the presence of sunlight for 72 hours and imaged again for evidence of GFP quenching.

Hatching and rearing of mosquitoes

Mosquitoes were reared and maintained at 27°C ± 0.5, 80% ± 2 RH, and a 16:8 hr (light:dark) photoperiod with a 1hr brown-up and brown-down to simulate dawn and dusk. Colonized *Ae. agypti* and *Ae. albopictus* eggs were reared as previously described (Bowers et al., 1995). Females were placed into cohorts of fifty at 5-7 days post-emergence, allowing time for females to have mated; males were disposed.

Virus infection of mosquitoes

Cohorts of fifty females, 5-7 days post-emergence were caged together for 48 hours, deprived of carbohydrates for 24 hours, and proffered a viremic bloodmeal to infect mosquitoes with SINV through the oral route of infection. Eighteen ml warmed (37°C) defibrinated bovine blood (Colorado Serum Inc. CO) and 2ml TR339 at a titer of 10^8 PFU/ml was added to a small collagen sausage casing for an overall titer of 10^7 PFU/ml TR339. For fluorescence; 1ml TR339 TaV-eGFP (William Klimstra, University of Pittsburgh) was added to blood to make a 10ml bloodmeal with titers ranging from 2.25×10^5 to 1.35×10^7 PFU/ml virus suspensions. The filled collagen casings were presented to the mosquitoes for one hour as previously described by Lyski and colleagues (2011). After 1 hour the mosquitoes were briefly chilled and engorged females were separated from unfed females. Engorged females were gently returned to cages for further analysis and nonfed females discarded.

Morphology and gut ultrastructure

Midguts were resected from *Ae. aegypti* and *Ae. albopictus* at day 7 p.i., and split into anterior midgut, posterior midgut, and hindgut. Tissue was then fixed for 48 hours with 2% gluteraldehyde and 0.1% tannic acid in 0.1M cacodylate buffer (pH 7.4) at 4°C. A secondary fixation with 1.0% OsO_4 for 30 minutes was applied and then dehydrated via increasing (30%, 50%, 70%, 95%, 100%) concentrations of ETOH washes then put into propylene oxide transitional fluid. Samples were then embedded into Epon 812 resin with a 3:7 ratio of NMA: DDSA for a slightly softer than medium hardness of resin (Luft, 1973). For light level analysis, sections were cut at 1-2 microns and stained with 0.1% methylene blue (pH 11) for 90 seconds on a hotplate. For STEM analysis gold-silver

ultrathin sections were cut and strained with uranyl acetate and lead citrate (Miller et al., 1993).

Scanning electron microscopy of midgut basal lamina surface

The midgut of an adult *Ae. albopictus* female unbloodfed and allowed to mate was resected onto a piece of carbon tape on an aluminum stub in PBS. No chemical fixation was used and the midgut was immediately placed into an environmental scanning electron microscope (ESEM). Images were taken using a large field detector and chamber pressure around 1 Torr. One tracheole was chosen and a series of high resolution images were taken and stitched together using Photoshop.

Confocal analysis of guts and salivary glands

Midguts of bloodfed *Ae. aegypti* mosquitoes were dissected over a time-course from 1 to 11 days p.i. with both gut and salivary glands (SG) sampled at day 30 p.i. Dissections were made directly onto a microscope glass slide via butt pull or while submerged under chilled PBS. The butt-pulled guts were immediately fixed via submerging in chilled 4% paraformaldehyde in 0.1M Cacodylate buffer for 5 minutes followed by applying cover slips using VECTASHIELD Mounting Medium from Vector Labs (https://www.vectorlabs.com/catalog.aspx?prodID=427). Guts and SG dissected under PBS were transferred to chilled 4% paraformaldehyde for 5 minutes and then placed into handmade wells of 60% glycerol and cover slipped. Selected samples were stained with DRAQ5 for 5-10 minutes prior to mounting. Samples were then viewed via an Olympus FluoView1000 confocal microscope for presence of GFP and evidence of virus.

Leg assay and measure of cytopathic effect (CPE)

At days 7, 9, and 12 p.i. of TR339 challenged mosquitoes, legs were removed and placed into cryovials and stored in a -20°C freezer. For fluorescence, legs were sampled for each resected gut. BHK-21 cells were cultured at 37°C in EMEM, supplemented with 20µg/ml Gentamycin and 2.5 µg/ml Amphotericin-B. Preconfluent BHK-21 cells in 6 well plates were challenged with a single leg and scored for the absence or presence of CPE at 48 hours p.i. of BHK-21 cells. Detection of CPE in a leg assay is due to the presence of virus in the hemolymph and indicates disseminated virus outside the gut of the mosquito hemolymph.

Chapter 3: Results

Virus infection of invertebrate cell lines

Expression virus was adsorbed onto pre-confluent C7-10 cells for 1 hour on a platform rocker set on low speed at RT in 25 mm^2 flasks. Cells were washed once with PBS to clear inoculum and 3 mL of EMEM was added to flask that was then incubated at 37°C and 5% CO_2 for 24 hours. Parental expression virus, TR339 TaV-eGFP pass 1, and expression progeny virus, TR339 TaV-eGFP pass 2, were used to challenge C7-10 and C6/36 cell lines. Infected cells were detected by fluorescent expression of GFP at hours 0, 6, 12, 24, and 48 post infection (p.i.). Presence of GFP was observed initially at 6 hours p.i. with a growing infection perceived until reaching confluent fluorescence at 24 hours p.i. (Fig 2). Amount of fluorescence was calculated in ImageJ (NIH ver. 1.46r) by counting number of cells showing fluorescence divided by total number of cells in 10 random 100 um^2 squares (Table 1).
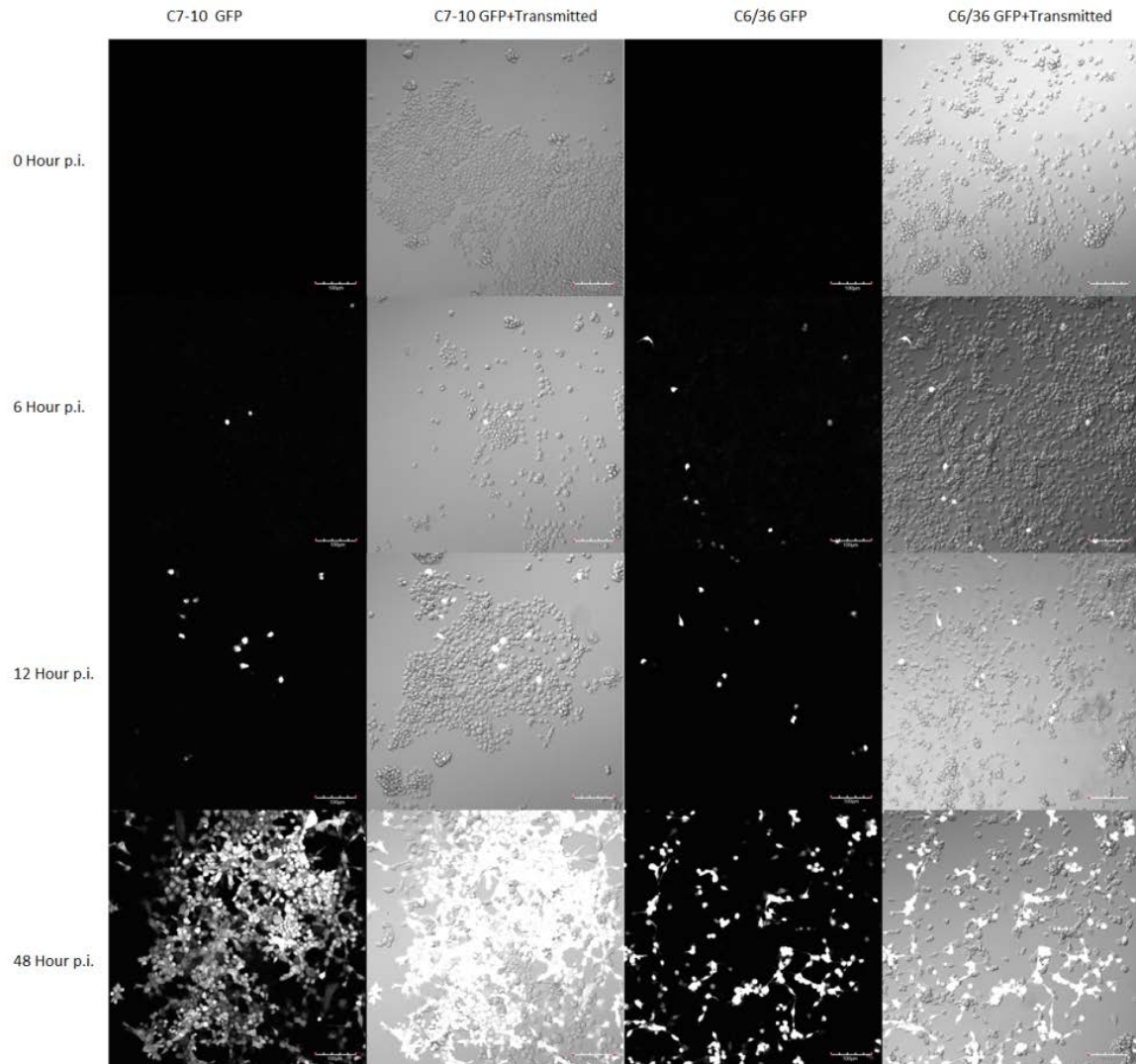
Figure 2. Fluorescent confocal images of C7-10 cells (Column I) and C6/36 cells
(Column III) infected with SINV TaV-eGFP at 0 hr, 6 hr, 12, and 48 hr p.i. Column II
and Column IV bright field overlay, respectively. 100µm scale bar.

Table 1. Percentage of infected cells versus total number of cells in C7-10 and C6/36 cells with both stock TR339 TaV-eGFP and passaged TR339 TaV-eGFP. Measurements were taken at a random selection of 10 100x100μm regions for each treatment.

Cell type	Virus	0 hours p.i.	6 hours p.i.	12 hours p.i.	24 hours p.i.	48 hours p.i.
C7-10	TR339 TaV-eGFP pass 1	0%	3%	4%	18%	82%
	TR339 TaV-eGFP pass 2	0%	1%	7%	20%	75%
C6/36	TR339 TaV-eGFP pass 1	0%	3%	3%	8%	34%
	TR339 TaV-eGFP pass 2	0%	2%	5%	7%	13%

Virus titer and fluorescence in progeny expression virus

Expression virus was previously passaged once in the vertebrate cell line, BHK-21. Expression virus was further serial passaged four times in BHK-21 cells to bring the expression virus to its 5th passage in a vertebrate cell line. Titration of passaged expression virus was calculated using plaque assays on BHK-21 cells (Table 2). At 18 hours p.i. for each plaque assay, plaques were viewed for fluorescence of GFP (Fig 3). Titration was shown to increase to titers greater than $1x10^8$ PFU/mL, required for *per os* infection of mosquitoes, while retaining the GFP fluorescent tag.

Table 2. Titration of virus replication and expression of GFP for TR339 TaV-eGFP over

5 passages in BHK-21 cells. (+) indicates presence of GFP in infected cells.

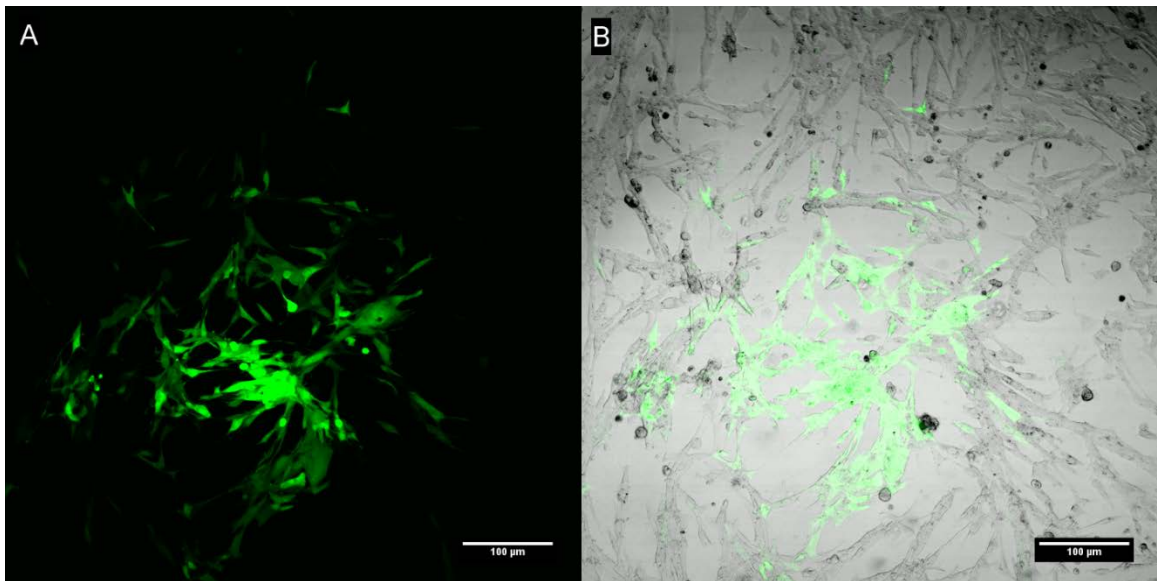| Starting titer (PFU/ml)	MOI (PFU/cell)	Passage titer (PFU/ml)	Passage #	GFP expression
2.3×10^6	0.0375	3.0×10^8	2	+
3.0×10^8	14.9	1.0×10^9	3	+
1.0×10^9	50	1.3×10^{10}	4	+
1.3×10^{10}	640	1.5×10^8	5	+

Figure 3. Fluorescent confocal image (A) and bright field overlay (B) of a virus plaque in

BHK-21 cells at 18 hours p.i. Plaque is visualized by expression of GFP in infected cells

surrounded by clear uninfected cells. 100µm scale bar.

Quenching challenge of GFP in infected invertebrate cells

Cells infected with TR339 TaV-eGFP were fixed for 30 minutes with 4% paraformaldehyde in 0.1 M Na cacodylate buffer; leakage of GFP was not observed following chemical fixation (Fig. 4). Cells were then placed under the 488nm Argon laser, GFP excitation wavelength, for 30 minutes and then re-exposed to the beam once every 30 minutes for 24 hours. Infected cells still showed strong fluorescence (Figs. 5 & 6). Cells were then left on a windowsill for 72 hours in direct sunlight and GFP still remained visible in infected cells (Fig 7).
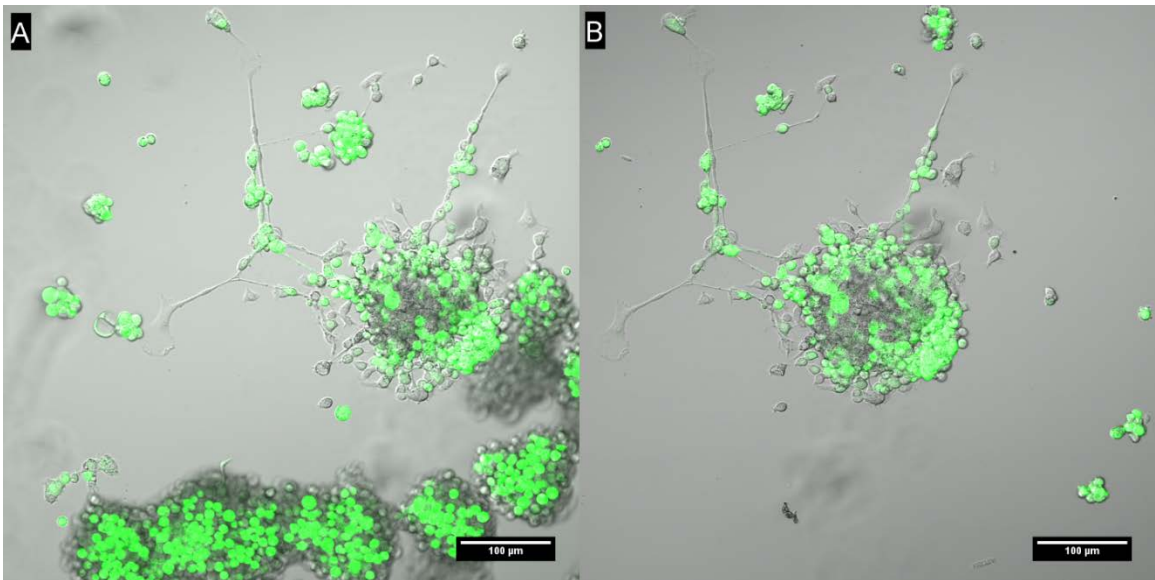

Figure 4. Fluorescent confocal image with LSM overlay of infected C7-10 cells pre (A) and post (B) fixation in 4% paraformaldehyde. 100µm scale bar.
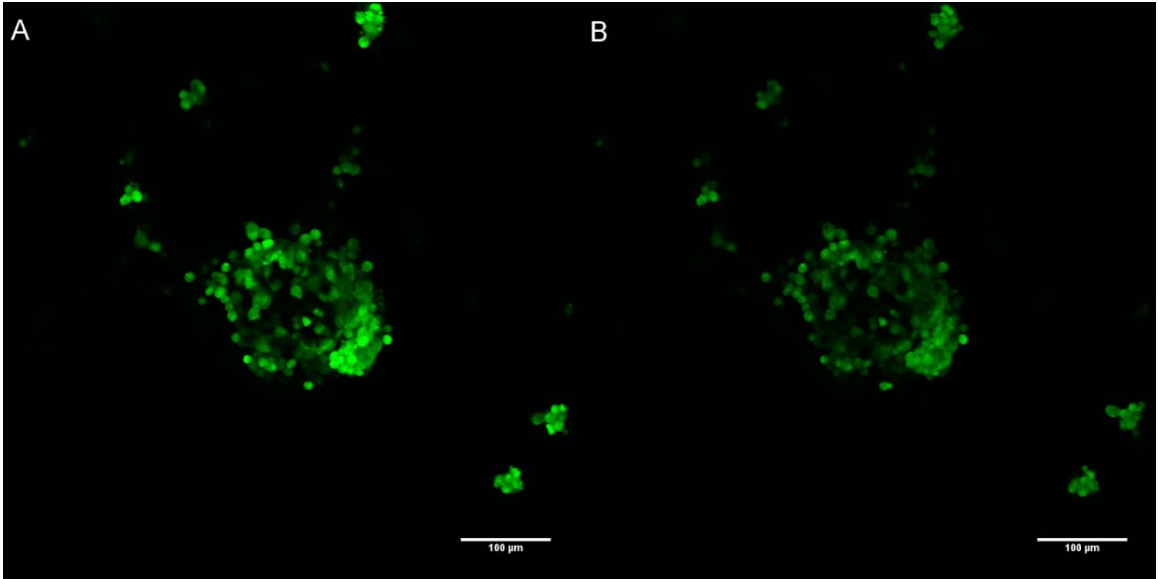
Figure 5. Fluorescent confocal images of paraformaldehyde fixed infected C7-10 cells before (A) and after (B) treatment of 30 minute continuous scanning with 488nm Argon laser. 100µm scale bar.
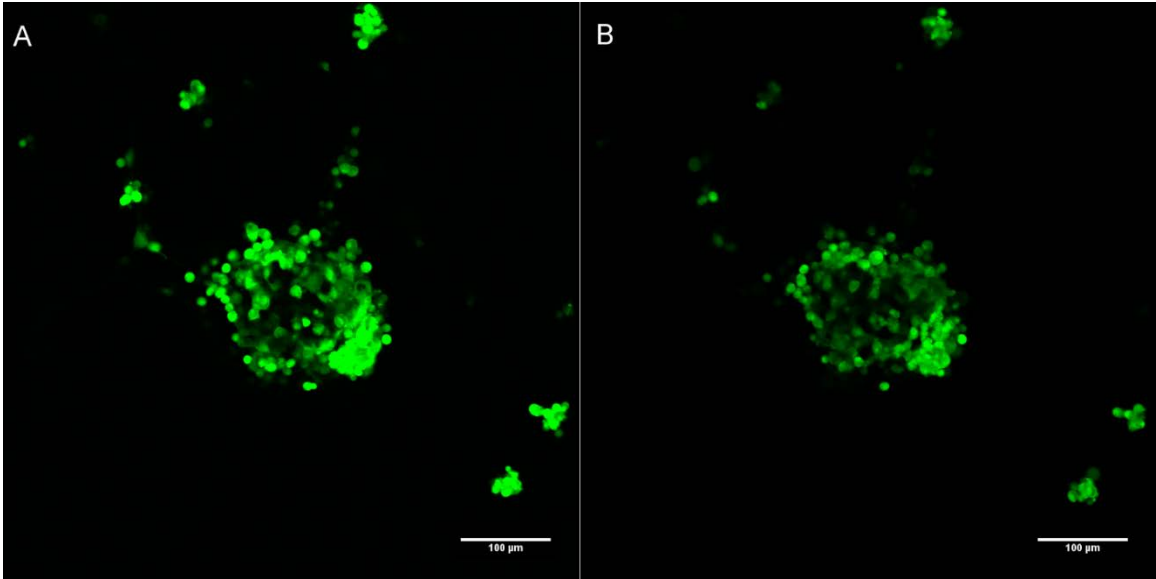
Figure 6. Fluorescent confocal image of paraformaldehyde fixed infected C7-10 cells before (A) and after (B) treatment of 20 hour scanning with 488nm Argon laser every 30 minutes. 100µm scale bar.
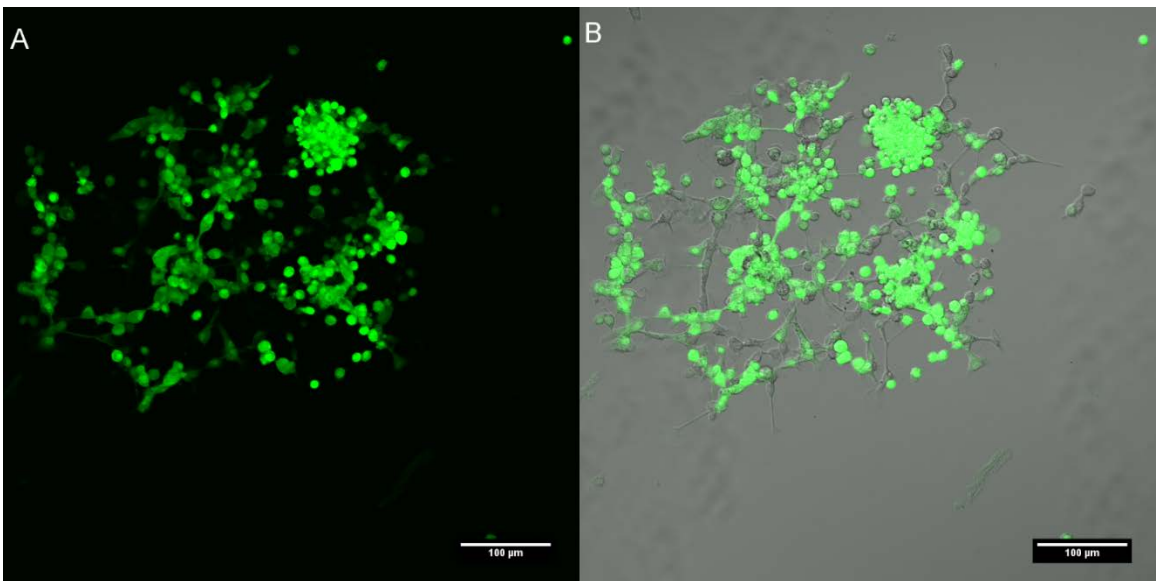

Figure 7. Fluorescent confocal image (A) and bright field overlay (B) of paraformaldehyde fixed infected C7-10 cells after 72 hours of access to direct sunlight. 100µm scale bar.

Structural response of gut to non bloodfed/bloodfed/viremic bloodfed

   Aedes aegypti mosquitoes were split into three cohorts: nonbloodfed, bloodfed,

and viremic bloodfed with TR339. Whole guts were dissected at day 7 p.i. and sectioned

into anterior midgut (AMG), posterior midgut (PMG), and hindgut (HG). Samples were

then fixed in 2% gluteraldehyde in Na cacodylate buffer and secondarily fixed in 1%

OsO_4 and embedded in Epon 812. Blocks were sectioned on an ultramicrotome (Sorvall-

Porter MT2). Differential staining and long wispy microvilli can be seen in the AMG and

PMG (Figs. 8 & 9). The HG shows a classic brush border (Fig. 10). The trachea and

muscle bundles attach to the thick basement membrane (Figs. 11 & 12). Physiological

evidence of digestion following a bloodmeal was observed in the PMG and not in AMG

or HG; muscles show some disorganization when fed viremic bloodmeal (Table 3, Fig.

13). A comparison study in *Ae. albopictus* shows less distension due to a bloodmeal (Fig.

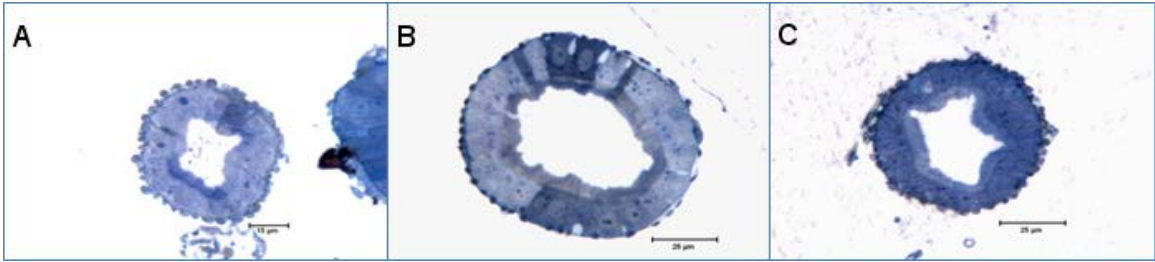14). Legs assayed showing dissemination as early as day 7 p.i. (Table 4)

Figure 8. Semithin cross-section of AMG for nonblooded (A), bloodfed (B), and viremic bloodfed (C). Basal surface of the AMG is covered with longitudinal muscle segments. Differential staining of cells can be seen in the nonblooded and bloodfed segments. Bloodfed AMG is significantly distended when compared to nonblooded AMG. There is an increased disorganization in microvilli caused by this distention. Microvillar height is also noted to be longer than the classic brush border found in other digestive epithelial tissue.

Figure 9. Semithin cross-section of PMG for nonbloodfed (A), bloodfed (B), and viremic bloodfed (C). Basal surface of the PMG is covered with longitudinal and circular muscle segements. There is a noticeable distention of the PMG in response to a bloodmeal. Additionally there appears to be a lack in relaxation of muscle segments in response to the viremic bloodmeal. Microvillar height is noted to be longer than the classic brush border. The microvilli also show disorganization in bloodfed PMG when compared to nonbloodfed PMG.
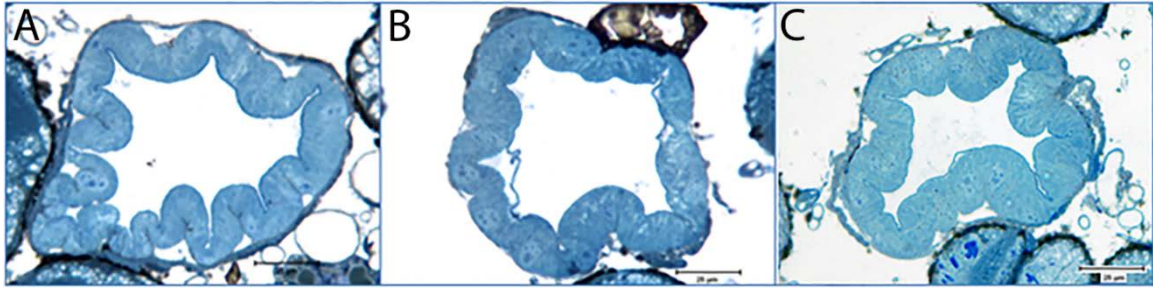
Figure 10. Semithin cross-section of hindgut (HG) for nonbloodfed (A), bloodfed (B), and viremic bloodfed (C). A classic brush border appearance of microvilli is visible which supports the function of the hindgut as mainly expulsion instead of digestion. Circular and longitudinal muscle bands are visible as well has some tracheoles. Malpighian tubule cross-sections and ovaries are visible along the edges of the images. There is little visible difference between nonbloodfed and bloodfed HG.

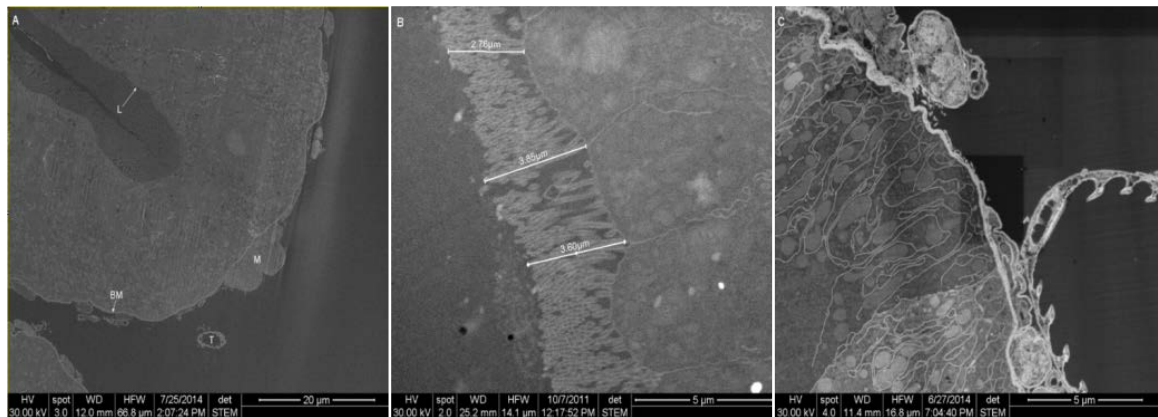Figure 11. STEM cross-section of *Ae. aegypti* midgut. (A) Low magnification image showing cross section from lumen (L) to the basement membrane (MB) with several longitudinal muscle bundles (M) and trachea (T). (B) Heavy distribution of microvilli line the lumen of midgut epithelial cells. (C) Basal lateral aspect showing basal infoldings of cell membrane deep into the cells and thick electron-dense BM.

Table 3. Average length of microvilli and inner circumferential length in PMG across nonbloodfed, bloodfed, and viremic bloodfed treatments. Inner circumferential length measured according to interface between microvilli and luminal membrane.

Treatment	Microvilli length (um)	StdErr	Inner Circumferential length (um)	StdErr
Nonblooded	5.21	0.17	1087	112
Bloodfed	5.86	0.33	1022	148
Viremic bloodfed	5.57	0.32	1246	179

Figure 12. Electronmicrograph of the basal lamina surface (hemolymph) of *Ae.*
albopictus midgut. Prominent tracheoles, as well as circular and longitudinal muscle
bands are visible. Whole-mount fresh tissue without chemical fixation was observed.
Images were taken at 10kV using a large field detector (LFD) at a chamber pressure of
0.974 torr and room temperature. Insert is a higher resolution image demonstrating the
branching of the tracheoles into small diameter tracheoles and circular muscle fiber.

Figure 13. Semithin cross-section of *Ae. aegypti* PMG for nonblooded (A-C), bloodfed (D-F), and viremic bloodfed (G-I). Stained with methylene blue and imaged with LSM. Differentially stained cells are noted more in the nonblooded guts while the blooded guts appear more distended. Viremic bloodfed guts are more heavily in-folded and lumen collapsed compared with mock bloodfed in 2 of the samples. 100µm scalebar.
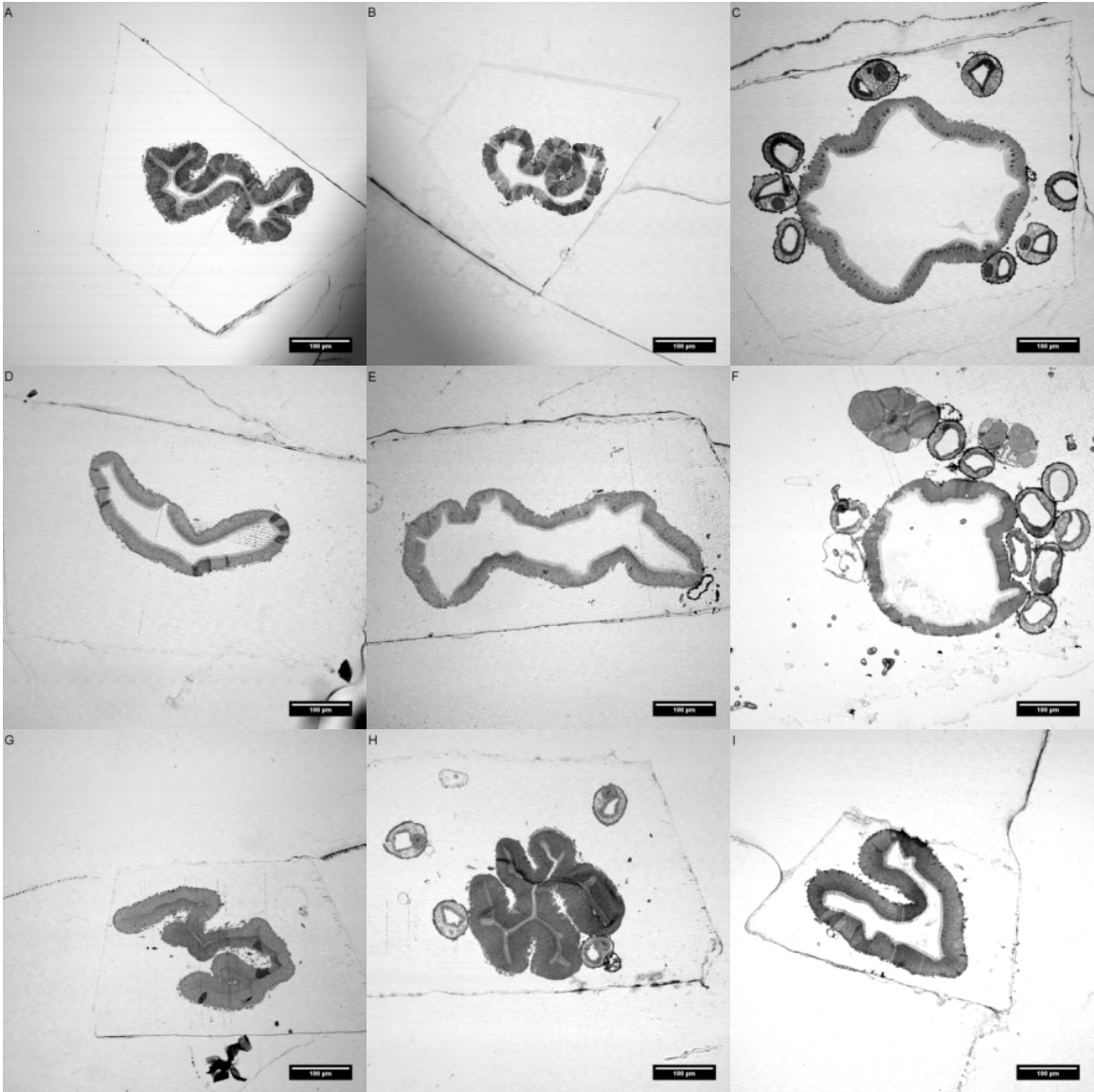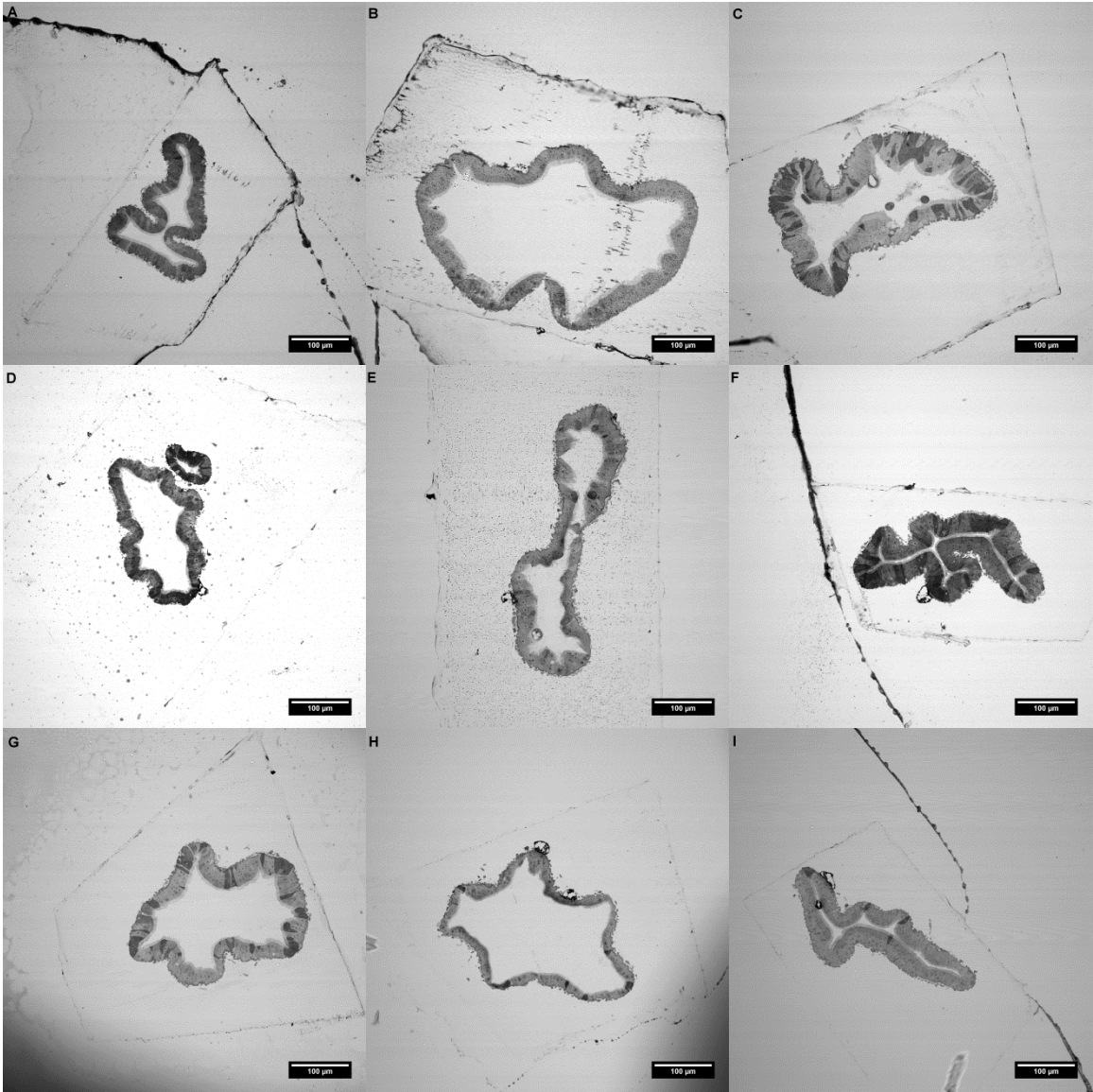
Figure 14. Semithin cross-section of *Ae. albopictus* PMG from nonblooded (A-C), bloodfed (D-F), and viremic bloodfed (G-I) adult female mosquitoes. Stained with methylene blue and imaged with LSM. 100µm scalebar.

Table 4. Dissemination based on leg assay(# disseminated/ # mosquitoes fed) from TR339 stock infected *Ae. aegypti* and *Ae. albopictus*. No data for days 9 and 12 with *Ae. albopictus*.

	Day 7	Day 9	Day 12
Ae. aegypti	1/9	1/5	0/5
Ae. albopictus	1/5	-	-

Mosquito midguts infected per os with expression virus

     Aedes aegypti adult female mosquitoes were fed expression virus at day's 5-10 post-emergence. Guts were either dissected directly onto glass microscope slides via a butt-pull method or dissected under PBS and placed into handmade wells filled with 60% glycerol in DI water and coversliped. Legs were taken for CPE leg assay to determine dissemination of virus. Infections of midguts were localized via GFP fluorescence. At day 3 p.i. a small focus of GFP presenting cells was observed in the epithelial cells of the gut (Fig. 15). At day 5 p.i. the area of GFP presenting cells covered approximately 50% of the gut (Fig. 16). This suggest cell-to-cell spread of the infection cell-to-cell. There was a difference seen between the butt-pull and under solution resection techniques seen in day 5 p.i. infections (Fig. 17). Peristaltic muscle cells intimately associated with the outside of the infected guts did not display any fluorescence at days 3 and 5 p.i. as well as negative leg assays, together indicative of a lack of dissemination (Table 5).
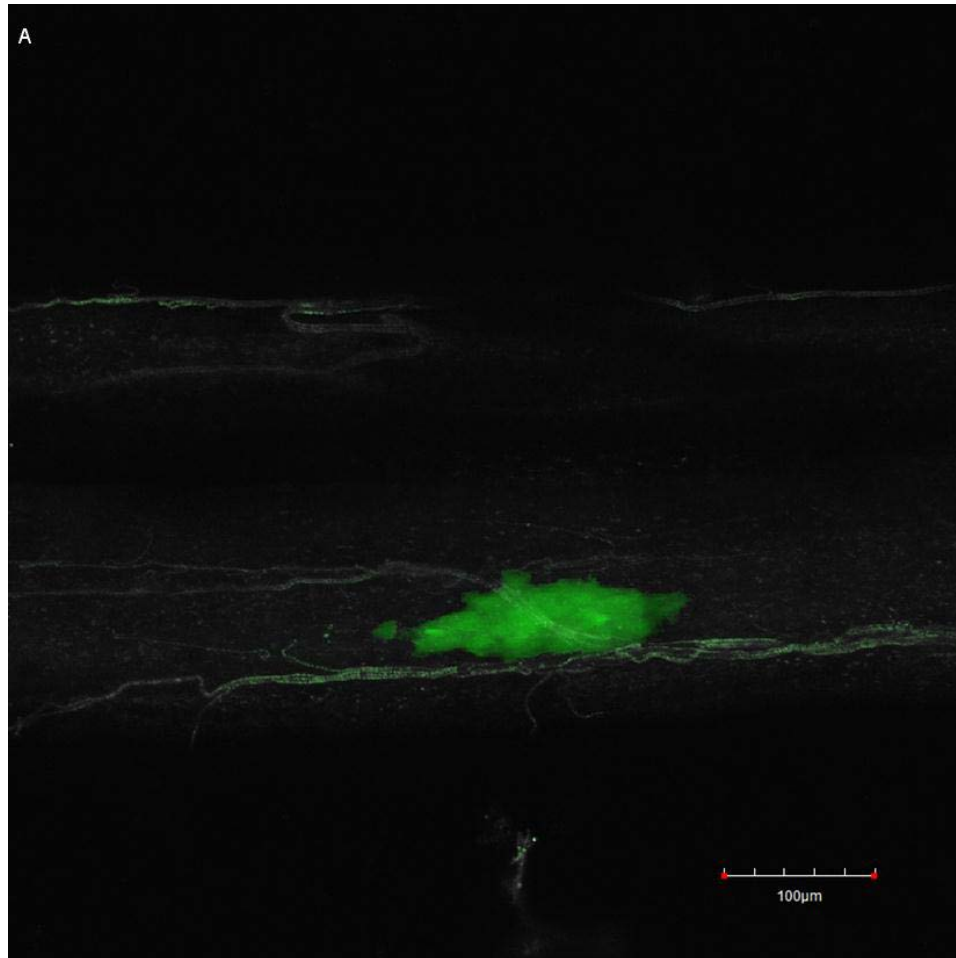
27

Figure 15. Fluorescent confocal image of *Ae. aegypti* midgut infected with SINVTaV-GFP at day 3 p.i. Localized foci of infection is observed in MG epithelial cells. 100μm scale bar.
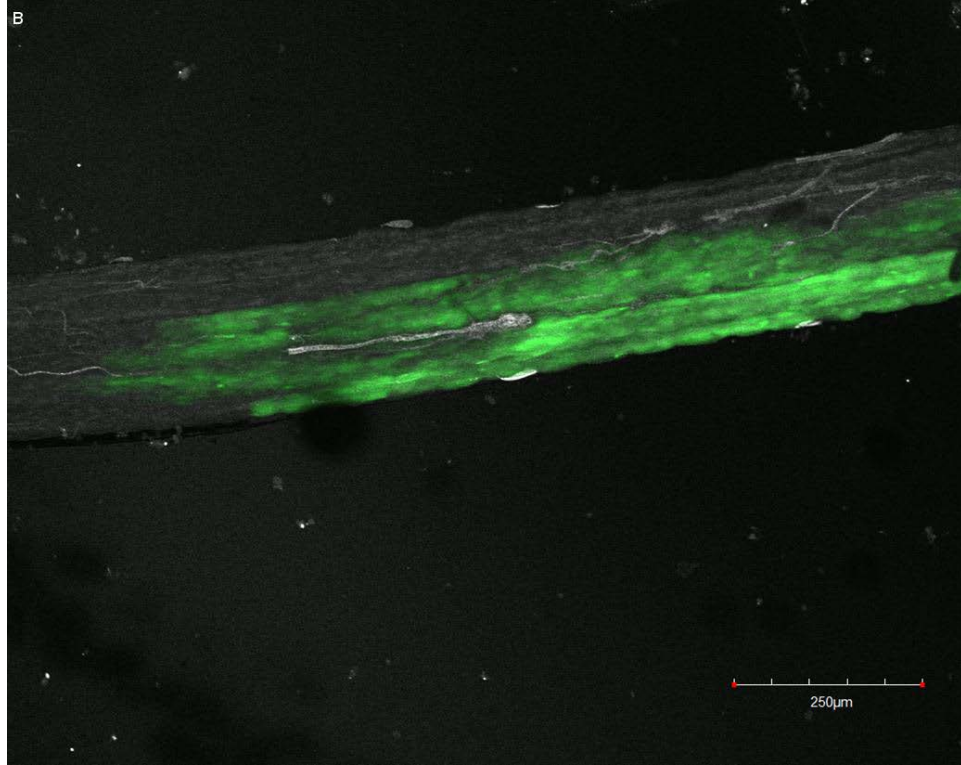
Figure 16. Fluorescent confocal image of *Ae. aegypti* midgut infected with SINVTaV-GFP at day 5 p.i. Larger area of infection probably due to cell-to-cell spread of virus observed. 150µm scale bar.
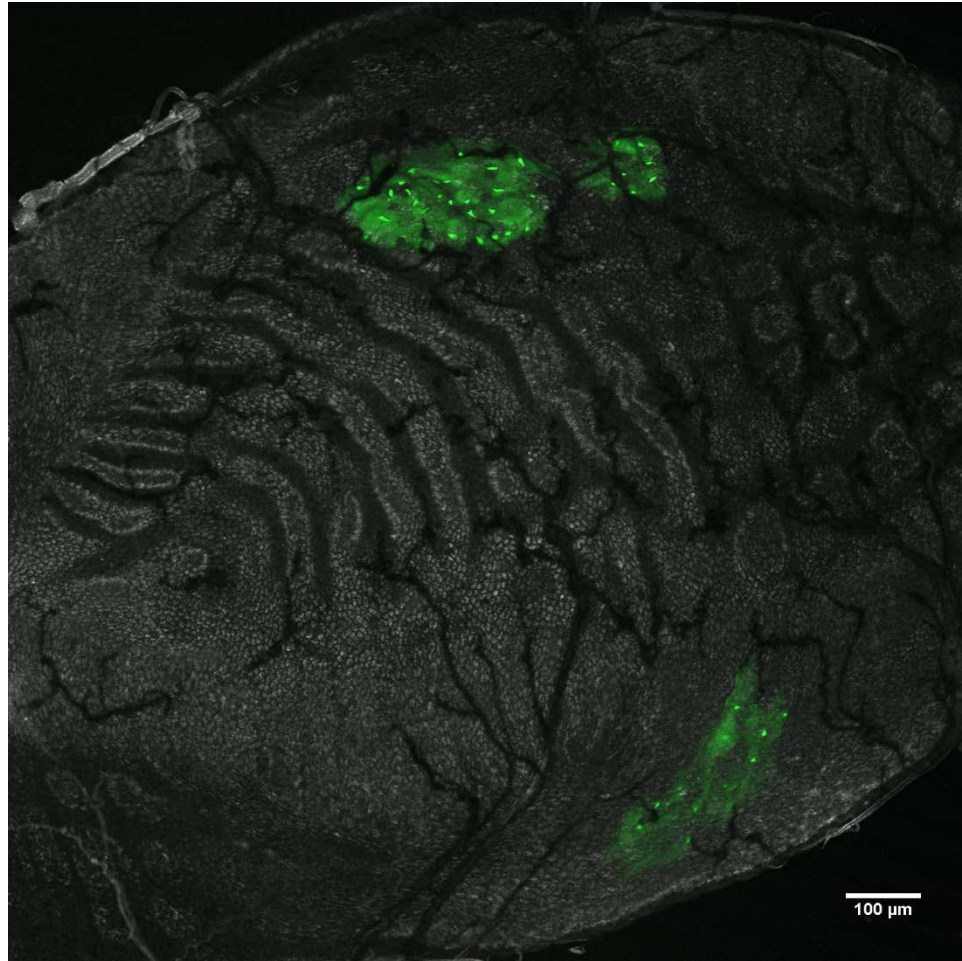
Figure 17. Fluorescent confocal image of *Ae. aegypti* midgut infected with SINVTaV-GFP at day 5 p.i. via resection under PBS fluid method. Three distinct foci of infection are evident as varying sizes. Concentrations of GFP in the foci are potentially infected entroendocrine cells. 100µm scale bar.

Table 5. Midgut infection of TR339 TaV-eGFP bloodmeals and dissemination via leg assay.

Bloodmeal titer (PFU/ml)	Midgut infection (%)		Dissemination (%)
2.25×10^5	8.0%	(2/25)	0.0%
2.25×10^5	0.0%	(0/12)	0.0%
9.9×10^6	3.7%	(1/27)	0.0%
1.35×10^7	13.3%	(2/15)	0.0%

Disseminated infection

Disseminated virus was observed in mosquitoes at 30 days pi. Guts, legs, and SGs were removed. Localized foci of infection in gut were identified (Fig. 18). In the SG GFP was seen in the proximal lateral lobe with gross pathology in the distal lateral lobe (Fig 19). Virus was not detected in the medial lobe.
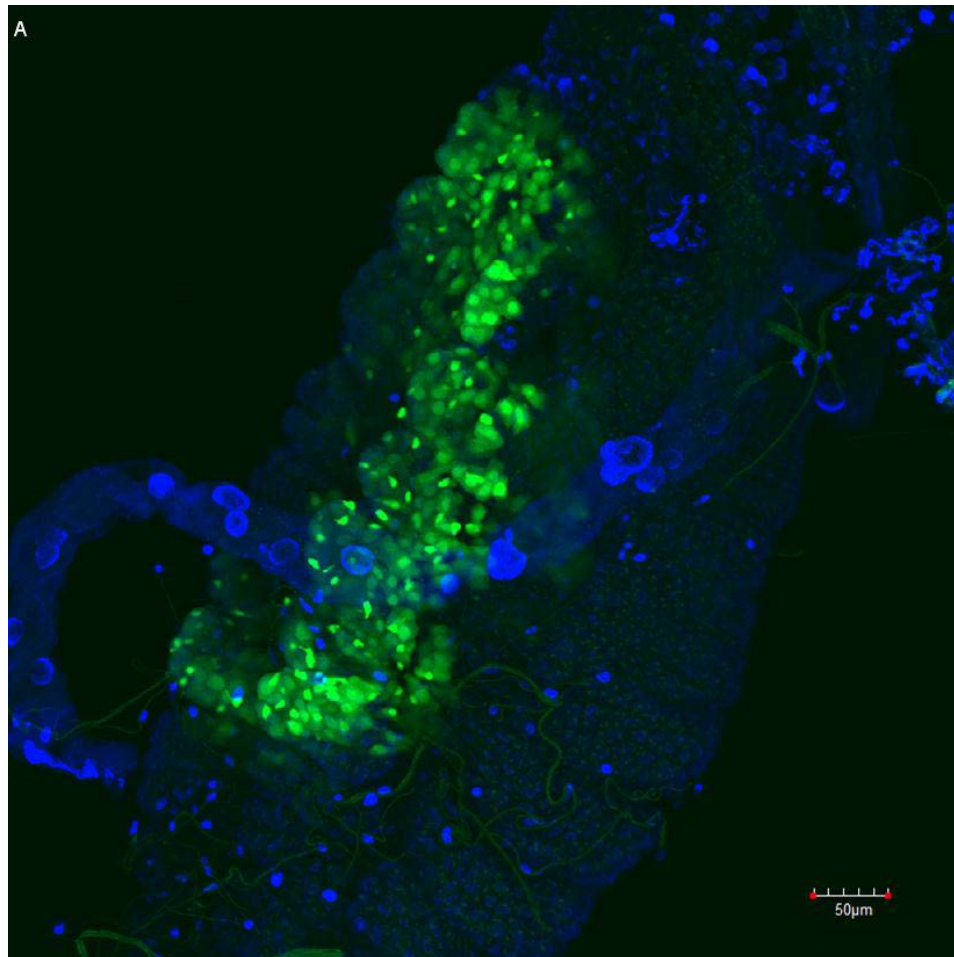
Figure 18. Fluorescent confocal image of *Ae. aegypti* midgut at day 30 p.i. [green GFP, blue DRAQ5] . A single virus focus is localized to the epithelium and muscle bundles are not identified. One Malpighian tubule is draped across the gut structure. 50µm scale bar.

Figure 19. Fluorescent confocal image with bright field overlay of *Ae. aegypti* SG at day

30 p.i. Persistence of expression virus localized in SG proximal lateral (PL) lobe at day

30 p.i. Gross cytopathology observed in distal aspect (DL) of the infected lateral lobe.

The medial lobe (ML) was refractory to infection. 50μm scale bar.

Chapter 4: Discussion

The initiative for the cell culture experiments in this investigation was due to a lack of expression protein seen in initial attempts to feed *Ae. albopictus* an expression virus, SVHR-GFP, that was a double promoter tag. It raised the following concerns to address:

1. mutational loss of the expression protein complex

2. the inability of mosquito cells to maintain the expression of the protein

3. quenching of the expression signal over the period of days in the mosquito and during the dissection itself under the dissecting microscope lamp

4. choice of fixation of the tissue allowing the expression protein to 'bleed out' or turning the protein off

Hence cell culture experiments were designed to determine whether the expression virus was able to infect mosquito cell lines and if so, then if the expression protein was still fluorescent after dissection and fixation of infected tissue with the new SINV TaV-GFP expression virus.

It was demonstrated that virus will infect two different strains of *Ae. albopictus* cells, C7-10 and C6/36, with both a first passage and second passage virus. Initial detection of GFP was seen at 6 hours. Initial budding of E2 is known to occur in chicken embryo fibroblasts at 2-3 hr p.i. with matured virions starting to bud at 4-5hr p.i., with maximal production closer to 6-8hr p.i. (Birdwell and Strauss, 1974, Pierce et al., 1974). Thus the expression of GFP in infected cells seen as early as 6 hr p.i. shows the potential for expression of GFP to show up within the first round of infection, tagging the initial

infection sites. The percentage of GFP stained cells continued to increase throughout the 48 hour study, indicating good retention of the expression protein within an invertebrate cell line. The C6/36 cells were slower to start which may be caused by a lower density of cells as they did not plate on the glass cover slip as densely as C7-10 cells. The brightness of the GFP expression in the invertebrate line is well above background, suggesting that the expression of GFP being produced in this manner will be clearly visible in tissue.

The retention of the expression protein in vertebrate cell lines was investigated. TR339 is known to acquire heparan-sulfate receptor mutations in a low number of passages in BHK cells (Klimstra et al., 1998). The expression virus was passaged 4 times in BHK cells in this lab without diluting the progeny virus between passages to replicate infection in a host. Titers increased in each passage to useable concentrations (Pierro et al., 2007) without loss of expression protein which is consistent with previous work (Sun et al., 2014). On the fifth passage there was a drop in titer either corresponding to a change from T-25 to T-75 flasks used to increase volume yield or established cyclic titer variations with high MOIs (Johnston et al., 1975).

An aside observation was made during the double overlay plaque assays for calculating progeny virus. A normal plaque assay technique requires several days to prepare and read the assay. After the initial infection of the cell monolayer for SINV it takes between 2-3 days before plaques of sufficient size and displaying CPE to develop. A further 12-24 hours is required with the second neutral red overlay to clearly differentiate the uninfected cells from the plaques with CPE in order to quantify the number of plaques and get a titer calculation. With the use of this expression virus, flasks were observed as early as 6 hours p.i. with the initial formation of plaques glowing with

the expression protein. It was trivial to quantify the plaques and get a titer for the virus within 12 hours of starting the assay allowing the eventual plaque to grow in size in order to avoid missing it upon observation. Another advantage to this method is the size of the plaques are small enough to allow for a higher density of plaques to be counted whereas with the double overlay method at 2-3 days p.i. the plaques would have grown into each other leading to miscounts. Besides a quicker assay time, this leads to higher confidence in an accurate reading.

During dissections it is possible that infected tissue will be under a bright dissecting lamp and under fixatives. Fixation used for gut resections is chilled 4% paraformaldehyde to retain cellular and membrane integrity. How well a mosquito cell will line retain the GFP reporter during this process was examined. C7-10 cells were incubated for 72 hr p.i. with the reporter virus. Confocal microscopy checked that the majority of cells were expressing the reporter and still attached to the flask. The cells were then washed with PBS and fixed for 30 minutes in chilled 4% paraformaldehyde. Re-imaging the same field of view post fixation showed the infected cells still attached to the flask did not lose the reporter protein, while loose cells were washed away. The cells were then left exposed to laser light at the excitation wavelength for GFP for 30 minutes and then for 20 hours. While there was a decrease in intensity after both trials, the expression was still well above background. The cells were then left on a window sill with direct sunlight for 72 hours. The original field of view couldn't be relocated but infected cells showing clear expression of GFP were imaged. This shows the hardiness of the chosen expression protein, eGFP, to handle a fixation regiment and presentation of light that exceeds to what resected tissues will be exposed. It is assumed then that special

conditions will not be required during dissections in order to maintain the visible level of fluorescence with confidence.

The mosquito gut is a cell monolayer with three regions of structural and functional differences along the longitudinal axis. These three regions of the gut have three different functions which are reflected by the gross morphology and makeup of the composite cells. The anterior region (foregut) is primarily used as a conduit of the bloodmeal to the posterior midgut. The diameter of the gut in this region is smaller than the midgut and heavily covered in longitudinal muscles. As such it was not expected to see much of a difference between treatments. The hindgut finishes adsorption and expulsion of the bloodmeal, having classic brush border microvilli and closely associated circumferential muscles (Vo et al., 2010). Again no difference between treatments was expected and semithin sectioning of these regions of the gut revealed no structural difference between treatments.

The posterior midgut region acts as the traditional stomach of the mosquito, as such it expands to hold the bloodmeal and is heavily covered in muscles and tracheoles. Semithin sectioning of these regions in *Ae. aegypti* showed disorganization in the elongated microvilli and distension in the bloodfed treatments. Two of the guts of the virus treatment group showed in folding of the epithelium but verification of infection was not possible. This pattern was not observed in the *Ae. albopictus* midguts. This shows potential promise of a morphological difference in SINV infected midguts with *Ae. aegypti*, but the experiment needs to be redeveloped with controls for verifying viral infection in the gut as well as ensuring sections are being taken through regions that are infected.

Three total blood feeds to investigate early time points p.i. were conducted with expression SINV and *Ae. aegypti* mated adult female mosquitoes. *Aedes aegypti* was the mosquito of choice because they are easy feeders compared to *Ae. albopictus*. The first barrier the virus encounters in the luminal epithelial lining of the midgut, where there is a thick layer of microvilli and the formation of a peritropic membrane. While the exact mechanism of infection is unclear, SINV antigens have been shown to be evident in localized patches of epithelial cells in the midgut (Ciano, 2010; Pierro et al., 2007). Furthermore it has been speculated that biochemical processes in the epithelial cells lining the midgut restricts the ability of the virus to infect other midgut cells along the luminal surface (Pierro et al., 2007). It was to be expected then to see localized infection of midgut epithelial cells. Fluorescence at day 3 p.i. was seen to be a single focus. At day 5 p.i. the infection covered a larger portion of the gut but still was seen to start from a small finite number of initial sites. Negative leg assays show that this infection is evident prior to dissemination of SINV into the hemolymph. This follows directly with previous results of SINV antigens found in localized isolated patches in *Ae. aegypti* (Lyski, 2013). It is evident that utilizing TaV tagging mimics natural infection of the wild type virus closely in *Ae. aegypti*.

Two methods of dissection were used to accomplish gut resections. When the guts were resected while submerged in chilled PBS there appeared concentrations of GFP. Initially these regions look non-cellular compared to epithelial digestive cells of the gut, something supported by the size of GFP, 26.9 kDa (Tsien, 1998) or potential charge (Tsvetkova et al., 2013). Further investigation with the nuclear stain, DRAQ5, showed that these regions have small nuclei located more basal to the gut lining with processes

that extend out towards the apical surface. The morphology of these cells suggest them to be enteroendocrine cells (Brown et al., 1995). Work is planned to verify these are enteroendocrine cells via immunohistochemistry and direct labeling of virus to see if SINV is highly concentrated in these cells. This may also suggest the site of amplification and eventual escape for disseminated virus as the basal morphology of such cells are modified compared to other epithelial digestive cells (Brown et al., 1995).

In order for an infected mosquito to be capable of transmitting virus by bite, the SG must be infected. These bilateral tri-lobed glands synthesize and release a large repertoire of secretory products (Almeras et al., 2010; Kelly et al., 2012). An established infection in these glands allows for the transmission of the virus during the suck-and-spit behavior when imbibing a bloodmeal (Clements, 1996). It has been previously demonstrated in Aedine mosquitoes that a persistent infection of SINV is localized to the lateral lobes of the SG not the medial lobe (Ciano et al., 2014). In addition gross pathology is found in the distal lateral lobes leaving the proximal lateral lobe intact. This allows for the SG to retain function so the now infectious mosquito can imbibe more bloodmeals. Guts and SG were dissected at day 30 p.i. with expression virus and secondarily labeled with DRAQ5. Infected guts showed evidence that the infection in the midgut epithelial cells remained localized while SG showed gross pathology in a distal lateral lobe with expression of GFP localized to the adjoining proximal lateral lobe. The expression of GFP therefore lasted 30 days in a live host and followed previous work on the location of persistent infection of wild type SINV. Furthermore there seemed to be no ill effect to the mosquito host, making this a promising route for further investigation of

mosquito-host interactions without the need for costly and time intensive immunohistochemistry techniques.

The present investigation has shown good retention of the expression of TR339 TaV-eGFP in both mosquito cell lines C7-10 and C6/36 and adult female *Ae. aegypti* and *Ae. albopictus* midgut and SG tissues. In general the infection pattern follows established literature for wild-type SINV. The establishment of a titration protocol with fluorescent-tagged virus improves upon the standard plaque assay for a quicker and more accurate titration without moving to more complicated genomic techniques. This suggests TaV tagging of the SINV genome with a small fluorescent probe to be a beneficial tool in studying the infection of SINV in the mosquito host. Further work is planned to study TR339 TaV-eGFP in other mosquito species and tissues.

References

Abell, B.A., and D.T. Brown. 1993. Sindbis virus membrane fusion is mediated by reduction of glycoprotein disulfide bridges at the cell surface. Journal of Virology. 67(9):5496-5501.

Almeras, L., A. Fontaine, M. Belghazi, S. Bourdon, E. Boucomont-Chapeaublanc, B. Orlandi-Pradines, T. Fusai, C. Rogier. 2010. Salivary gland protein repertoire from *Aedes aegypti* mosquitoes. Vector Borne Zoonotic Dis. 10;391-402.

Alto, B.W., L.P. Lounibos, and S.A. Juliano. 2003. Age-dependant blood feeding of *Aedes aegypti* and *Aedes albopictus* on artificial and living hosts. J. Am. Mosq. Control Assoc. 19:347-352.

Birdwell, C.R., and J.H. Strauss. 1974. Replication of Sindbis Virus IV. Electron Microscope Study of the Insertion of Viral Glycoproteins into the Surface of Infected Chick Cells. Journal of Virology. 14(2):366-374.

Bowers, D.F., B.A. Abell, and D.T. Brown. 1995. Replication and tissue tropism of the alphavirus Sindbis in the mosquito *Aedes albopictus*. Virol. 212:1-12.

Bowers, D.F., C.G. Coleman, and D.T. Brown. 2003. Sindbis virus-associated pathology in *Aedes albopictus* (Diptera:Culicidae). J. Med. Entomol. 40(5): 698-705.

Breitbart M., and F. Rohwer. 2005. Here a virus, there a virus, everywhere the same virus?. Trends Microbiol. 13(6):278–84.

Brown, M.R., A.S. Raikhel, and A.O. Lea. 1985. Ultrastructure of midgut endocrine cells in the adult mosquito, *Aedes aegypti*. Tissue & Cell. 17:709-721.

Caley, I.J., M.R. Betts, N.L. Davis, R. Swanstrom, J.A. Frelinger, and R.E. Johnston. 1999. Venezuelan equine encephalitis virus vectors expressing HIV-1 proteins: vector design strategies for improved vaccine efficacy. Vaccine. 17(23):3124-3135.

Chamberlain, R.W., and W.D. Sudia. 1961. Mechanism of transmission of viruses by mosquitoes. Ann. Rev. Ent. 6:371-390.

Ciano, K.A. 2010. Temporal and biochemical aspects of Sindbis virus dissemination in the mosquito host. UNF Thesis and Dissertations. 67. http://digitalcommons.unf.edu/etd/67/

Ciano, K.A., J.J. Saredy, and D.F. Bowers. 2014. Heparan Sulfate Proteoglycan: An Arbovirus Attachment Factor Integral to Mosquito Salivary Gland Ducts. Viruses. 6(12):5182-5197.

Clements, A.N. 1996. The Biology of Mosquitoes, Adult food and feeding mechanisms. Champman and Hall London. p 222.

Gratz, N.G. 2004. Critical Review of the vector status of *Aedes albopictus*. Med. Vet. Entomol. 38:215-227.

Hardy, J.L., W.C. Reeves, and R.D. Sjoren. 1976. Variations in the susceptibility of field and laboratory populations of *Culex tarsalis* to experimental infection with western equine encephalomyelitis virus. Am. J. Epidem. 103:498-505.

Houk, E.J. 1977. Midgut ultrastructure of *Culex tarsalis* (Diptera:Culcidae) before and after a bloodmeal. Tissue & Cell 9(1):103-118.

Johnston, R.E., D.R. Tovell, D.T. Brown, and P. Faulkner. 1975. Interfering Passages of Sindbis Virus: Concomitant Appearance of Interference, Morphological Variants, and Truncated Viral RNA. Journal of Virology. 16(4):951-958.

Kelly, E.M., D.C. Moon, and D.F. Bowers. 2012. Apoptosis in mosquito salivary glands: Sindbis virus-associated and tissue homeostasis. Journal of General Virology. 93(11):2419-2424.

Klimstra, W.B., K.D. Ryman, and R.E. Johnston. 1998. Adaption of Sindbis virus to BHK cells selects for use of heperan sulfate as an attachment receptor. Journal of Virology. 72(9):7357-7366.

Luft, J.H. 1973. Embedding Media — Old and New. Advanced Techniques in Biological Electron Microscopy. pp. 1-34.

Lyski, Z.L., J.J. Saredy, K.A. Ciano, J. Stem, and D.F. Bowers. 2011. Blood feeding position increases success of recalcitrant mosquitoes. Vector-Borne and Zoonotic Diseases. 11(8): 1165-1171.

Lyski, Z.L. 2013. Arbovirus persistence and selection of persistent variants following chronic infection in Aedine mosquitoes: a comparative study between *Ae. aegypti* and *Ae. albopictus* 30 days post infection with Sindbis virus. UNF Thesis and Dissertations. 430. http://digitalcommons.unf.edu/etd/430/

Miller, M.L., and D.T. Brown. 1993. The distribution of Sindbis virus proteins in mosquito cells as determined by immunofluorescence and immunoelectron microscopy. J. Gen. Virol. 74: 293-298.

Moore,C.G., and C.J. Mitchel. 1997. *Aedes albopictus* in the United States: ten-year presence and public health implications. Emergy Infect Dis. 3:329-334.

McKnight, K.L., D.A. Simpson, S. Lin, T.A. Knott, J.M. Polo, D.F. Pence, D.B. Johannsen, and H.W. Heidner. 1996. Deduced consensus sequence of Sindbis virus strain AR339: mutations contained in laboratory strains which affect cell culture and *in vivo* phenotypes. Journal of Virology. 70(3):1981-1989.

O'Meara, G.F., L.F. Evans, Jr., A.D. Gettman, and J.P. Cuda. 1995. Spread of *Aedes albopictus* and decline of *Ae. Aegypti* (Diptera:Culicidae) in Florida. J. Med. Entomol. 32:554-562.

Okuda, K., F. de Almeida, R.A. Mortara, H. Kriegar, O. Marinotti, and A.T. Bijovsky. 2007. Cell death and regeneration in the midgut of the mosquito, *Culex quinquefasciatus*. Journal of Insect Physiology. 53:1307-1315.

Pierce, J.S., E.G. Strauss, and J.H. Strauss. 1974. Effect of Ionic Strength on the Binding of Sindbis Virus to Chick Cells. Journal of Virology. 13(5):1030-1036.

Pierro, D.J., E.L. Powers, and K.E. Olson. 2007. Genetic determinants of Sindbis virus strain TR339 affecting midgut infection in the mosquito *Aedes aegypti*. Journal of General Virology. 88:1545-1554.

Renz, D. and D.T. Brown. 1976. Characeristics of Sindbis virus temperature-sensitive mutants in cultured BHK-21 and *Aedes albopictus* (mosquito) cells. Journal of Virology. 19(3): 775-781.

Romoser, W.S., L.P. Wasieloski Jr, P. Pushko, J.P. Kondig, K. Lerdthusnee, M. Neira, and G.V. Ludwig. 2004. Evidence for Arbovirus Dissemination Conduits from the Mosquito (Diptera: Culicidae) Midgut. J. Med. Entomol. 41(3):467-475.

Singh, K.R.P. 1967. Cell cultures derived from larvae of *Aedes albopictus* (Skuse) and *Aedes aegypt*i (L). Curr. Sci. 36:506-508.

Shahabuddin, M. and P.F. Pimenta. 1998. *Plasmodium gallinaceum* preferentially invades vesicular ATPase-expressing cells in *Aedes aegypti* midgut. Proc. Natl. Acad. Sci. 95:3385-3389.

Strauss, J.H, and E.G. Strauss. 1994. The alphaviruses: gene expression, replication, and evolution. Microbiol. Rev. 58:491-562.

Sun, C., C.L. Gardner, A.M. Watson, K.D. Ryman, and W.B. Klimstra. 2014. Stable, High-Level Expression of Reporter Proteins from Improved Alphavirus Expression Vectors To Track Replication and Dissemination during Encephalitic and Arthritogenic Disease. Journal of Virology. 88(23):2035-2046.

Taylor, R.M., T.H. Hurlbut, J.R. Work, J.R. Kingston, and T.E. Frothingham. 1955. Sindbis virus: newly recognized arthropod transmitted virus. Am. J. Trop. Med. Hyg. 4:844-862.

Tsien, R.Y. 1998. The green fluorescent protein. Annu. Rev. Biochem. 67:509-544.

Tsvetkova, I.B., F.Cheng, X. Ma, A.W. Moore, B. Howard, S. Mukhopadhyay, and B. Dragnea. 2013. Fusion of mApple and Venus fluorescent proteins to the Sindbis virus E2 protein leads to different cell-binding properties. Virus Research. 177(2):138-146.

Vo, M., P.J. Linser, and D.F. Bowers. 2010. Organ-Associated Muscles in *Aedes albopictus* (Diptera:Culicidae) Respond Differentially to Sindbis Virus. J Med Entomol. 47(2):215-225.

Wang, G. 2008. Sindbis Virus Interaction with Cells. North Carolina State University, Raleigh, NC. http://repository.lib.ncsu.edu/ir/bitstream/1840.16/4270/1/etd.pdf

Watson, D.G., J.M. Moehring, and T.J. Moehring. 1991. A mutant CHO-K1 strain with resistance to *Pseudomonas* exotoxin A and alphaviruses fails to cleave Sindbis virus glycoprotein PE2. Journal of Virology. 65(5):2332-2339.

Zieler, H., C.F. Garon, E.R. Fischer, and M. Shahabuddin. 1998. Adhesion of *Plasmodium gallinaceum* ookinetes to the *Aedes aegypti* midgut: sites of parasite attachment and morphological changes in the ookinete. J. Euk. Microbiol. 45:512-520.

Zieler, H., C.F. Garon, E.R. Fischer, and M. Shahabuddin. 2000. A tubular network associated with the brush-border surface of the *Aedes aegypti* midgut: implications for pathogen transmission by mosquitoes. The J. of Exp. Biology. 203: 1599-1611.

Vita

Jason Jonathan Saredy

EDUCATION

Masters of Science in Biology

University of North Florida   Jacksonville, FL   April 2015

Bachelors of Science in Physics

Bachelors of Science in Mathematics

University of North Florida   Jacksonville, FL   December 2010

RESEARCH

Laboratory Technician - Dr. Spaulding, Engineering Fellow

Vistakon, Jacksonville, FL   April 2013 – Current

- Set up, operation, and maintenance of internal, custom laboratory instruments. Write testing protocols and execute tests against said protocols while ensuring accurate documentation and dissemination to relevant teams. Support the development and validation of new and novel optical performance metrics.

- Write and support a cross-language software library for 2d phase unwrapping of data from a polarized Twyman–Green interferometer utilizing IDL, Python, C, and VBA

Research Assistant - Dr. Bowers, Professor Biology

University of North Florida, Jacksonville, FL   May 2005 – Current

- Maintenance mosquito insectary. Installation and repair of humidification systems. Perform hatches and care to retain a viable supply of mosquitoes for arbovirus lab.

- Hatch, feed, and dissection of and preparation of mosquito midgut for ESEM, TEM, and Confocal analysis of trachea structure on midgut surface for viral dissemination pathways. Trained other personal on dissection and preparation of mosquito midgut.

- Utilization of invertebrate and vertebrate cell culture in support of viral stock maintenance and *in vitro* experimentation of fluorescent-tagged arboviruses.

- Rebuilt JEOL 35 CF SEM for use in a graduate course (MCB 6175C Integrative Microscopy). Repaired various aspects of the vacuum system, diffusion pump, rotary pumps, and electronics. Worked on and replaced electrical system.

- Use, maintenance, and training outside users on Olympus BX60 Epifluorescence microscope and Olympus FV1000 confocal microscope

Research Assistant - Dr. Patel, Senior Lecturer in Physics

University of North Florida, Jacksonville, FL   November 2004 – Jan 2013

- Fabrication, testing, and data analysis of thin film sensors. Fabrication using high vacuum thermal evaporation systems with both direct thermal and electron beam evaporation.

- Development of testing chambers from nominally toxic gases up to chemical warfare agents and explosives. Development of software to tie in data analysis hardware to testing chambers and circuitry in LabVIEW and VBA.

- Maintenance of specialized lab hardware: High impedance multichannel electrometers, gas injection systems, high vacuum thermal evaporation systems.

- Train new users on proper operation and supervise outside users on FEI Quanta 200 ESEM with EDAX.

- Maintenance on microscope including cleaning column, alignments, filament centering, and aperture replacement. In depth trouble shooting alongside FEI field technicians.

- Run analysis for users across various disciplines: material composition analysis, structural analysis, and biological applications.

TEACHING

Physics/Math Tutor

Tutor.com, New York, NY   Jan 2011 – Current

- Online tutoring for high school and introductory college classes in algebra and physics.

Graduate Teaching Assistant - Dr. Moon, Professor Biology

University of North Florida, Jacksonville, FL   Aug 2012 –April 2014

- Taught lab sections of 24 students each, providing additional teaching materials to back up introductory biology lectures while keeping a safe environment for students to perform experiments to also further their understanding of materials from their lectures.

- Taught 6 sections of General Biology 1 lab, 1 section of Anatomy & Physiology 2 lab, and 1 semester of prep work in support of Microbiology, Diagnostic Bacteriology, and Hematology lab courses

Physics/Math Tutor

Academic Center for Excellence – UNF, Jacksonville, FL   Jun 2005 – May 2009

- Group tutoring in both upper and lower division classes for mathematics, statistics, physics, chemistry, and computer science.

SKILLS

- Proficient in C, C++, BASIC, Visual BASIC, Visual C, HTML, SQL, JAVA, LabVIEW, Python, SciPy, VBA, R, and advanced hardware repair.

- Operation of various electron, light, and atomic microscopes, technician experience on FEI Quanta 200 ESEM and Olympus FluoView1000. Operation and repair of vacuum systems including roughing, diffusion, and turbo molecular pumps

- Cell culture in vertebrate and invertebrate cell lines. Experience working with a BSL-2 agent.

PAPERS

- "Isolation, Expression Analysis and Characterization of NEFA-interacting Nuclear Protein 30 and RING Finger and SPRY Domain Containing 1 in Skeletal Muscle", David S. Waddell, Paige J. Duffin, Ashley N. Haddock, Virginia E. Triplett, **Jason J. Saredy**, John T. Eldredge, and Karina M. Kakareka, Gene (In Review).

- "Heparan sulfate proteoglycan: an arbovirus attachment factor integral to mosquito salivary gland ducts", Kristen A. Ciano, **Jason J. Saredy**, and Doria F. Bowers, Viruses, November 2014, 6(12): 5182-5197.

- "Blood Feeding Position Increases Success of Recalcitrant Mosquitoes", Zoe L. Lyski, **Jason J. Saredy**, Kristen A. Ciano, Jenna Stem, and Doria F. Bowers, Vector Borne Zootic Diseases, August 2011, 11(8):1165-1171.

- "Odor Sensing with Indium Tin Oxide Thin Films on Quartz Crystal Microbalance", Nirmal Patel, Jay Huebner, **Jason Saredy**, Brian Stadelmaier, Sensors and Transducers Journal, April 2008, 91(4):116-126.

- "Measurement of the DC resistance of semiconductor thin film-gas systems: comparison to several transport models", Barbara Carrico, **J. Saredy**, J. L. Tracy, N. Patel, J. Garner and L. Gasparov, J. Appl. Phys., October 2007, 101.

PATENTS

- "Quartz crystal microbalance with nanocrystalline oxide semiconductor thin films and method of detecting vapors and odors including alcoholic beverages, explosive materials and volatilized chemical compounds", N. Patel, J. Huebner, B. Stadelmaier, J. Saredy US Patent #7930923 Filed April 1, 2009

POSTERS

- "Expression of TaV tagged Sindbis virus (TR339) in *Aedes albopictus* cell lines and adult mosquitoes"; J Saredy, D Bowers; Microscopy and Microanalysis 2014 *First Place Biology Student Poster*

- "Structural and ultrastructural features of the midgut of *Aedes aegypti* in response to blood meal an Sindbis virus infected blood meal", J Saredy and D. Bowers, University of North Florida S.T.A.R.S. Conference 2011

- "Midgut and Hindgut Ultrastructure Reflect Regional Functional Differences in the Mosquito *Aedes albopictus*", J. Saredy and D. Bowers, Sigma Xi Annual Meeting & International Research Conference 2010

- "Measurement of Ozone Profile in Stratosphere Using Nanocrystalline ITO Gas Sensor Arrays on High Altitude Balloon Platform", Nathan Walker, Bernadette

Quijano, Jason Saredy, Brain Stadelmaier, and Nirmal Patel, University of North Florida S.T.A.R.S Conference 2010

- "Towards the Development of Flexible Gas Sensor Arrays", Jason Saredy, Brain Stadelmaier, Jay Huebner, and Nirmal Patel, University of North Florida S.T.A.R.S Conference 2009

- "Detection of Explosive Materials Using Indium Tin Oxide on Quartz Crystal Microbalance Sensors", Jason Saredy, Brain Stadelmaier, Jay Huebner, and Nirmal Patel, University of North Florida S.T.A.R.S Conference 2009

- "Detection of Ozone Profile in Stratosphere Using Indium Tin Oxide Gas Sensors on High Altitude Balloon", Nathan Walker, Jason Saredy, and Nirmal Patel, University of North Florida S.T.A.R.S Conference 2009

- "Nanocrystalline enhanced oxide semiconductor sensor arrays for gases and vapors", Nirmal Patel, Jay Huebner, Jason Saredy, Brain Stadelmaier, Bernadette Quijano, Nathan Walker, Chemical and Biological Defense Science and Technology 2009

- "Fabrication of Acetylene Gas Sensors Using Nanocrystalline ITO Thin Films", Jason Saredy, Nirmal Patel, and Pearl Young, Jacksonville University 2006

TALKS

- "Measurement of the DC resistance of thin film semiconductor-gas systems: comparison to several transport models", J. Garner, B. Carrico, J. Saredy, J. L. Tracy, N. Patel, American Physical Society March Meeting 2007

SOCIETIES

- Society of Physics Students, American Physical Society, Sigma Xi, Microscopy Society of America, Sigma Pi Sigma